CFSRC COLLOQUIUM

Proceedings of the Cold-Formed Steel Research Consortium Colloquium
20-22 October 2020 (cfsrc.org)

Structure Performance of Cold-formed Steel columns reinforced by Channel Sleeve under Axial and Eccentric compression

Ziqi He [1], Qixiu Li [2], Ben Schafer [3], Xuhong Zhou[4]

Abstract

Due to the weak torsional stiffness of cold-formed thin-walled channel members, distortional buckling behavior maybe controlled the ultimate load-capacity under certain conditions. Therefore, a new section reinforced by Channel Sleeve is proposed in order to improve the structural capacity of channel columns in this paper and is performed on the axial and eccentric compression tests. The influence of Channel Sleeve spacing on the bearing capacity and failure mode is studied, and the beneficial effect of the Channel Sleeve on the bearing capacity is verified. First, the corresponding numerical modeling of the experiments is presented in detail by describing the numerical models, types of finite elements and methods of analyses. Second, the reinforced cold-formed steel members were subjected to axial and eccentric compression analysis. Next, the magnitude, direction of eccentricity and the sleeve position are varied, in order to address their effect on the columns' capacity and structural behavior. In addition, the numerical model is used to analyze the parameters such as the slenderness ratio of the specimen, the magnitude and direction of eccentricity. The influence of these parameter changes on the structural performance of the members under the action of axial and beam-column compression members is obtained. Finally, compare the bearing capacity of the axial compression specimen with the bearing capacity calculated by the North American Code.

1. Introduction

Cold-formed thin-walled channel members components are usually composed of C-section cold-formed steel and U-section cold-formed steel. Because of the open cross-section, they are prone to failure modes of local buckling, distortional buckling and global buckling when under load. when distortional buckling occurs, the flange and lip will rotate around the intersection of the flange and the web, which will reduce the bearing capacity of the component, so it needs to be prevented. A certain number of Channel Sleeves can be added to the single-limb column. The channel sleeve can effectively prevent the deformation of the opening section and can effectively improve the bearing capacity of the column. Multiple C-section cold-formed steel members and U-section cold-formed steel members can be used as the basic component units in the door and window opening side columns and other places that need to be reinforced. They are connected into cold-formed thin-walled steel built-up open-section components by self-tapping screws, which can greatly improve the bearing capacity of structural components and overcome the problem of insufficient bearing capacity of single limb components.

At present, scholars have studied some measures to control the distortional buckling of cold-formed thin-walled channel members. Demao Yang and Hancock[1] studied the performance of flanges and webs with V-shaped stiffening crimp channel steel axial compression members. Xiaotong Yang and Jian Yao[2] added diaphragms to cold-formed lipped channel columns and found that added diaphragms can improve the load capacity. Nuno Silvestre, Ben Young [3]conducted research on cold-formed steel columns reinforced by CFRP, and studied its bearing capacity and influence on buckling.

This paper proposes a reinforcement measure, which is to set up channel sleeve along the length of the column to restrain the rotation of the flange and the lip and control the occurrence of distortional buckling. The stability and bearing capacity of cold-formed steel columns reinforced by Channel Sleeve under axial and eccentric compression are simulated and analyzed by the finite element method, and on the basis of verifying the correctness of the model, the influence of the slenderness ratio, eccentricity and Channel Sleeves spacing on the compression performances of the Channel Sleeves reinforced type is studied.

[1] Associate professor, School of Civil Engineering, Chongqing University, Chongqing 400045, China
[2] Master student, School of Civil Engineering, Chongqing University, Chongqing 400045, China
[3] Professor, Department of Civil and Systems Engineering, Johns Hopkins University, Baltimore, MD 21218, USA
[4] Professor, School of Civil Engineering, Chongqing University, Chongqing 400045, China

2. Specimen Design and Finite Element Model

This paper will use ABAQUS finite element analysis software to simulate and analyze the axial and eccentric bearing capacity of the column with Channel Sleeves. The finite element analysis process is divided into two steps. First, perform eigenvalue analysis, and then perform eigenvalue analysis. Perform geometric nonlinear analysis to obtain the failure mode and ultimate bearing capacity of the specimen.

2.1 Specimen parameter

The thickness of the specimen is 2mm.The specimen subdivided into four column heights:400mm, 1000mm, 1600mm, 2200mm.The 400mm series specimens are not equipped with Channel Sleeve, 1000mm series specimens are equipped with a Channel Sleeve at one-half of the length, 1600mm series specimens are at one-third of the length and two-thirds of the length are respectively set up a Channel Sleeves, 2200mm series specimens are set at one-quarter length, one-half length, and three-quarter length are respectively set up a Channel Sleeve. The basic components are connected by self-tapping screws, and the dimensions of the test specimen are shown in Figure 1 and Figure 2. The screw spacing of the built-up channel columns with length of 1000mm, 1600mm and 2200mm is 300mm. For the built-up channel columns with length of 400mm the screw spacing is 150mm.Figure 3 is the naming convention of the specimen.

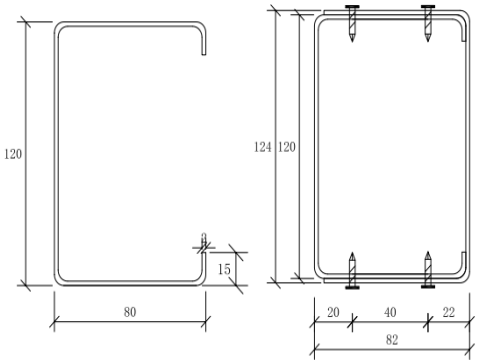

(a) (b)

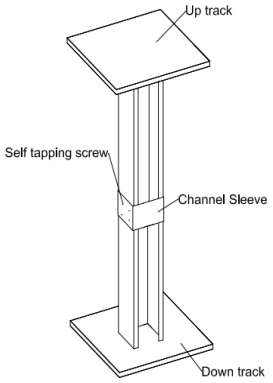

(c)

Figure 1: (a) Single-limb C-section, (b) C-section with the Channel Sleeve, (c) C-section 1000mm column

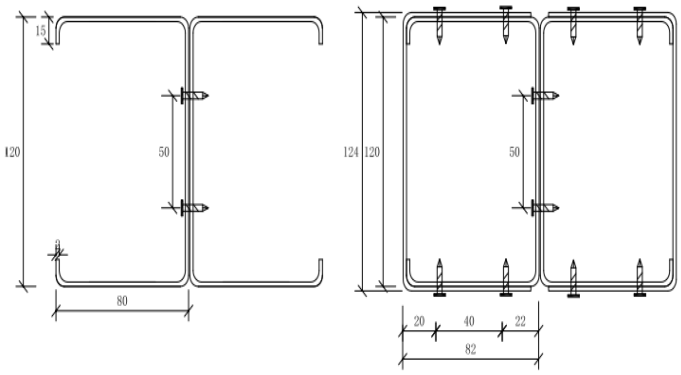

(a) (b)

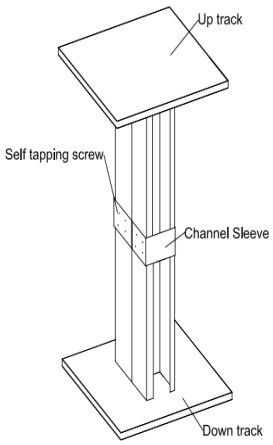

(c)

Figure 2: (a) Double-limb built-up section, (b) Built-up section with the Channel Sleeve, (c) Built-up section 1000mm column

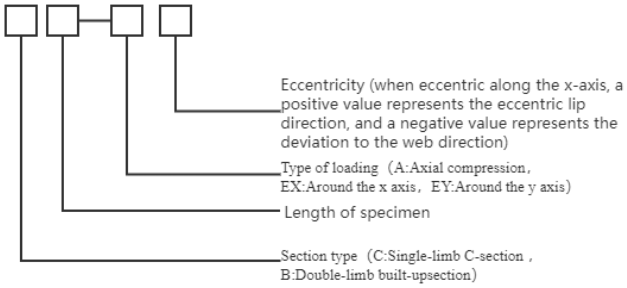

Figure 3: Cross-section types and naming convention

2.2 Finite element model element selection and meshing

In the finite element analysis model of this paper, the column and the Channel Sleeve are simulated by the four-node linear reduction integral element (S4R). Since the stiffness of the end plate is much larger than the stiffness of the specimen itself, in order to reduce the calculation, the end plate adopts discrete stiffness, and the displacement of the rigid body is determined by Reference point(RP) control . The size of the grid will affect the results of the finite element analysis. In order to make the calculation results more accurate and lower the calculation cost, the element size of the column is 10mm×10mm, the element size of the end plate is 20mm×20mm, and the size of the Channel Sleeve 5×5mm.

2.3 Boundary conditions and loading methods

In order to make the simulation conditions closer to the actual situation, for the specimens subjected to eccentric load, when the eccentricity is on the X-axis, the upper end of the fixed biased column except UR2 and U3, and the lower end of the UR2 are free to ensure that the biased column is only wound around When the Y-axis rotates, the displacement loading method is adopted. When the eccentricity is on the Y-axis, the upper end of the fixed biasing column is divided by UR1 and U3, and the lower end is divided by UR1. The displacement loading method is adopted. For specimens subjected to axial load, when the eccentricity is on the X-axis, the upper end of the fixed biased column except UR2 and U3, and the lower end of the UR2 are free, and the displacement loading method is adopted. In the nonlinear analysis, the load displacement according to Shafer's recommendation is generally 1.5 times the limit displacement.

2.4 Material properties and contact methods

The stress-strain curve of the steel in the finite element analysis in this paper adopts an ideal elastoplastic model, the yield strength is 345MPa, the Poisson's ratio is 0.3 and the elastic modulus is 2.06×10^5.

In the interaction module, the contacts and constraints between the parts are established, so that the created parts become a whole and can work together under force. The TIE constraint is adopted between the column and the end plate, so that the end plate and the column can be tightly connected together. Since the focus of this article is not the destruction of screws, the point-to-point coupling (coupling) is adopted, and the basic components are segmented according to the designed position in the part module. Coupling is set in the interaction module to connect C-C (that is two back-to-back The corresponding points of the C-section member) and C-U (that is the C- section member and the Channel Sleeve) are coupled together, and the degrees of freedom in each direction are restricted during coupling. A surface-to-surface contact is provided between the C-U and C-C components, the tangential direction is frictionless, and the normal direction is hard contact.

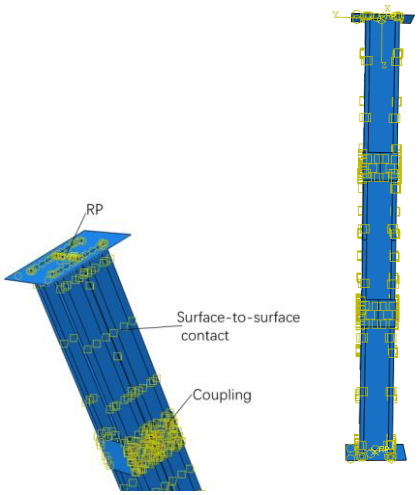

Figure4: Finite element model

2.5 Analysis process

First, perform characteristic buckling analysis to obtain the buckling mode of the entire component and its corresponding critical buckling load as the basis for introducing initial defects in the next nonlinear analysis. The study by Schafer et al.[4-6]shows that the cold bending effect and residual stress of steel during rolling. The residual stress has a small influence on the ultimate stress and can be ignored. The cold bending effect can increase the strength of the material by approximately 2%, but it can be ignored due to safety considerations. Non-linear buckling analysis is based on static analysis based on large deformation. The model in this paper has a large number of contact elements, which will lead to difficult convergence problems in the process of analyzing the model. Zhang and Young[7] suggest to introduce artificial damping. To ensure the accuracy of the calculation, Rusmmusen[8]

recommends 0.005 times the strain energy as the balance adjustment factor.

3. Parametric study

The study mainly focuses on the slenderness ratio, eccentricity, eccentricity direction of the specimen, and the influence of the Channel Sleeve on the ultimate bearing capacity.

3.1 Influence of column length

Change the length of the column, keep other parameters unchanged, and study the influence of the change of the column length on its axial compression performance. The columns' failure modes and ultimate load-bearing capacities under axial compression are presented in Table 1. Figure 5 shows the Load-axial displacement curves.

Table1: The ultimate load-bearing capacity of the specimens under the axial load

Specimen	P_A(kN)	Failure modes
C400-A	164.63	L
C1000-A	157.26	L
C1600-A	145.19	L+F
C2200-A	129.07	L+F
B400-A	316.05	D+L
B1000-A	333.65	D+L+F
B1600-A	318.12	D+L+F
B2200-A	290.81	D+L+F

*Note: D=distortional buckling; L=local buckling; F = flexural buckling

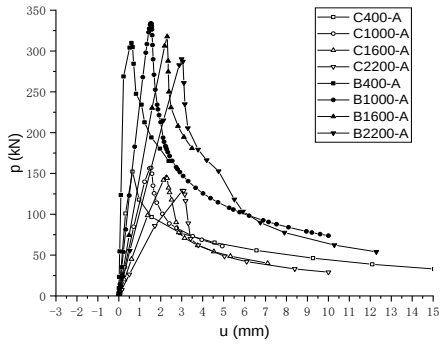

Figure 5: Load-axial displacement curves of columns with different length

From Figure 5 and Table 1, it can be seen that the bearing capacity of the single-limb C-section axial compression specimen with Channel Sleeve decreases as the length of the specimens increases. When the length of the specimen changes from 400mm to 2200mm, its bearing capacity force drop by 21.6%. The bearing capacity of the double-limb built-up open-section axial compression specimen decreases slightly with the increase of the specimen length, but it is not absolute. This is related to the failure mode of the specimen. Because the specimens mainly perform local and distortional interaction buckling mode, local buckling has a certain strength after buckling, so the change of length has little effect on the specimen. All the specimens suffered instability failure, and their ultimate bearing capacity was much smaller than the yield bearing capacity.

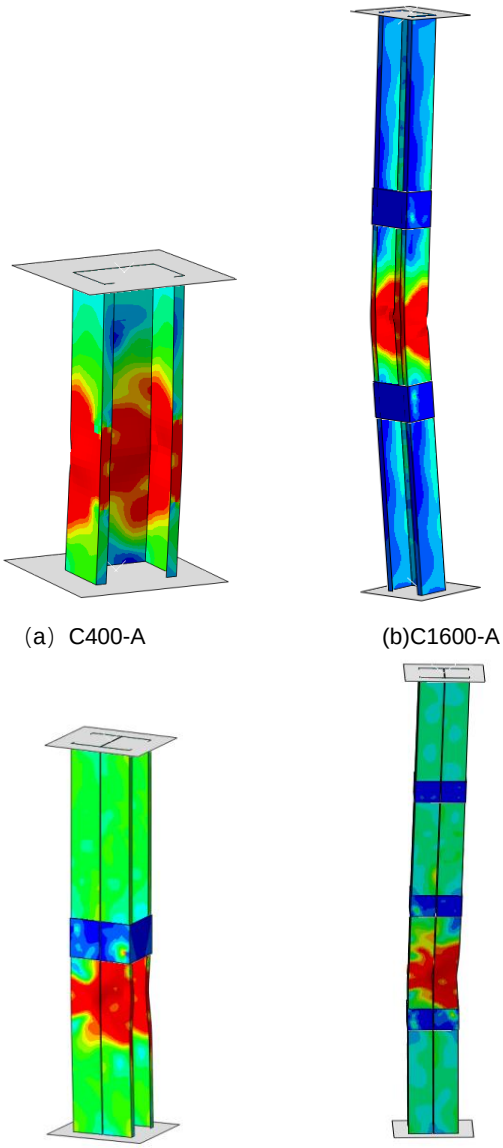

(a) C400-A (b)C1600-A

(c) B1000-A (d)B1600-A

Figure 6: Failure modes of partial specimens

3.2 Influence of eccentricity and eccentricity direction

For single-limb C-shaped cross-sections, there are three types of specimens: eccentricity about the weak axis (y-axis) in the direction of lip, eccentricity about the weak axis (y-axis) in the direction of the web, eccentricity around the strong axis (x axis) to the lip direction. For the built-up column, only the eccentricity of the specimen about the weak axis (y-axis)

in the positive direction and the eccentricity about the strong axis (x-axis) in the positive direction are studied.

The other parameters of the specimens remain unchanged, and the eccentricity in different directions are all set to 5mm,10mm, 20mm, 30mm, 40mm. Figure 7 shows the influence curve of the eccentricity and the eccentricity direction on the maximum bearing capacity of the specimen. Table 2 lists the ultimate load-bearing capacity of the biased series of specimens.

Table 2 and Figure 7 illustrate that when all specimens are subjected to eccentric load, their ultimate load-bearing capacity decreases with the increase of eccentricity. For a single-limb C-shaped section, when it is eccentrically compressed around the y-axis, When the eccentricity is 40mm, the ultimate load-bearing capacity of the specimen with a length of 2200mm decreases the most, which is 46.7% lower than that of the axial compression specimen. At this time, the specimen performs distortional buckling, and then occurs the flexural buckling around the weak axis. When it is eccentrically compressed around the x-axis, the ultimate load-bearing capacity of the 2200mm biased specimen decreases the most which is 57.4% lower than that of the axial pressure specimen. It's first appeared local buckling on the web, then the flange occurred local buckling, and then flexural buckling failure occurred. When it is compressed eccentrically around the x-axis, the bearing capacity of the 2200mm biased specimen decreases the most, which is 46.7% lower than that of the axial pressure specimen. The flange on the deviated side first performs local buckling. The increase of the specimen finally occurred flexural buckling failure around the strong axis.

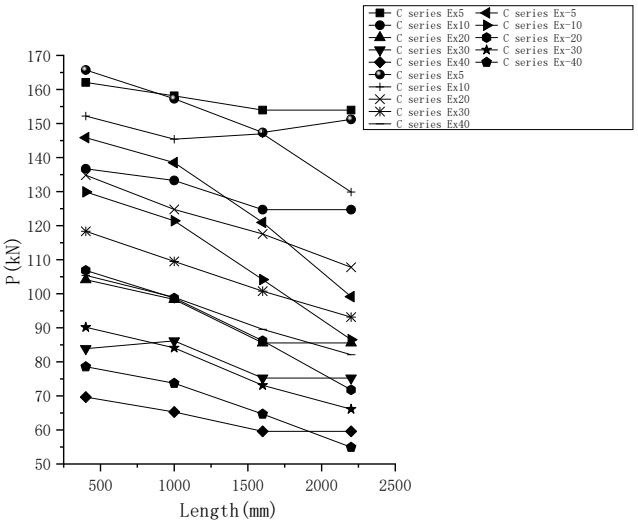

(a) Single-limb C-section specimens

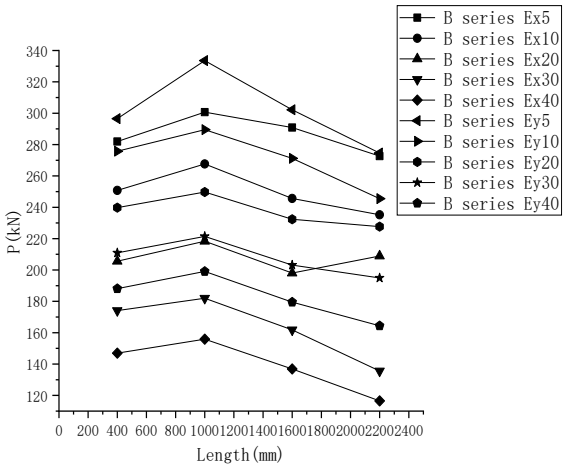

(b) Double-limb built-up specimens

Figure7: Relation curve of length and ultimate load-bearing capacity of specimens

For the built-up channel columns, When it is under eccentric load, the specimen will first appear distortional-local buckling interaction at the flange. As the load increases, the specimens with lengths of 400mm, 1000mm, 1600mm, and 2200mm will eventually undergo global buckling.

3.3 Influence of Channel Sleeves

The specimens C1000-A, C1000-Ex20, C1000-Ex-20, C1000-Ey20 were analyzed only by changing the distance between the Channel Sleeves, and the influence of the distance between the Channel Sleeves was studied. Table 3 lists the ultimate load-bearing capacity.

Table 3: Sample table of numbers

Specimen	Channel Sleeve spacing	P_A (kN)	The same cross-section specimen without Channel Sleeve (kN)
C1000-A-500	500	157.62	156.76
C1000-Ex20-500	500	98.47	93.52
C1000-Ex-20-500	500	98.69	99.53
C1000-Ey-500	500	124.77	123.75
C1000-A-333	333	161.45	156.76
C1000-Ex20-333	333	99.51	93.52
C1000-Ex20-333	333	98.63	99.53
C1000-Ey20-333	333	125.43	123.75
C1000-A-250	250	159.84	156.76
C1000-Ex20-250	250	105.35	93.52
C1000-Ex-20-250	250	99.94	99.53
C1000-Ey20-250	250	128.25	123.75

It can be seen from the table 3 that when the C1000 series specimen is under axial compression load, the setting of the

Channel Sleeves contributes little to the improvement of its bearing capacity, and it has almost no effect on the buckling mode of the column. As the Channel Sleeves distance decreases, its bearing capacity increases little. This is because the specimens are mainly subjected to local buckling when under the axial compression loads, and the existence of the Channel Sleeves has little effect on this type of buckling mode. When the specimen is eccentric 20mm around the strong axis and 20mm eccentric to the web around the weak axis, the increase in bearing capacity of the Channel Sleeves is also small. This is because under the action of these two types of eccentric loads, the specimen mainly occured local buckling and global buckling are dominant, and the Channel Sleeves has almost no effect on these two types of buckling modes. When the specimen is eccentrically curled around the strong shaft, when the hoop distance is 500mm, 333mm, and 250mm, its bearing capacity increases by 5.3%, 6.4%, and 12.6%, respectively. The failure mode of the specimen is distortional-global buckling interaction. The Channel Sleeves can better control the distortion and deformation of the specimens, so that the bearing capacity of the test piece has been greatly improved. When the Channel Sleeve distance is approximately one-third and a half wavelength, the bearing capacity increases the most.

3.4 The current direct strength method

Schafer [9] through a lot of research work, based on the research results of Hancock [10] on the Direct Strength Method of compressed columns, through statistical regression of a large number of test data, proposed the axial compression column and pure bending beam respectively The calculation formula of bearing capacity considering distortional buckling and local-total related buckling. At present, the direct strength method has been widely used in North America [11], Australia/New Zealand [12] and Brazil [13]

The comparative analysis of the maximum bearing capacity p_{nld} of the axial compression specimen calculated by the North American code and the finite element P_A is shown in the table 4. The calculation result of the North American code is more conservative than the finite element result. At present, there is no formula for calculating the bearing capacity of columns under eccentric loads in the North American code. At the same time, there is a lack of calculation formulas for the bearing capacity of compression columns with Channel Sleeve. In future studies, the calculation method of the ultimate bearing capacity of members under eccentric loads will be obtained.

Table 4: Finite element analysis result and DSM predictions for the columns

Specimen	P_A(kN)	P_{nld} (kN)	P_A / P_{nld}
C400-A	164.63	134.45	1.224
C1000-A	157.26	122.49	1.284
C1600-A	145.19	121.90	1.191
C2200-A	129.07	113.29	1.139
B400-A	316.05	277.77	1.138
B1000-A	333.65	270.15	1.235
B1600-A	318.12	252.13	1.261
B2200-A	290.81	230.69	1.261

7. Conclusions

This paper uses ABAQUS finite element software to analyze the bearing capacity and buckling mode of the compression column with Channel Sleeves. The analysis results show that the setting of Channel Sleeves can increase the bearing capacity of the compression column with distortional buckling, and the improvement of the bearing capacity increases as the distance between the Channel Sleeves decrease. However, the effect of improving the bearing capacity of the column with local buckling and flexura buckling is not significant.

The direct strength method formula in the North American code is used to calculate the bearing capacity of axial compression with Channel Sleeve, and the result is conservative. At present, the North American code lacks the direct strength method to calculate the bearing capacity of the column under the eccentric load, which needs to be obtained in future research.

8. References

[1] Demao Yang, Hancock, G, J. Numerical simulations of high strength steel lipped-channel columns[R]. R843.

[2] Xiaotong Yang, Jian Yao. Experimental study and finite-element analysis on Cold-formed channel column withconnecting cars between Lips [J]. Bulietin of Science and Technology, 2007, 23(5): 729-735.

[3] Nuno Silvestrea, Ben Youngb, Dinar Camotim. Non-linear behaviour and load-carrying capacity of CFRP-strengthened lipped channel steel columns[J]. Engineering Structures, 30 (2008) 2613–2630.

[4] Schafer B W, Pekoz T. Computational modeling of cold-formed steel: characterizing geometric imperfections and residual stresses[J]. Journal of Constructional Steel Research, 1998, 47(3): 193-210.

[5] Schafer B W, Li Z, Moen C D. Computational modeling of cold-formed steel[J]. Thin-Walled Structures, 2010, 48(10):752-762.

[6] Moen C D, Igusa T, Schafer B W. Prediction of residual stresses and strains in cold-formed steel members[J]. Thin-Walled Structures, 2008, 46(11):1274-1289.
[7] Zhang J.H., Young B. Numerical investigation and design of cold-formed steel built-up open section columns with longitudinal stiffeners [J]. Thin-Walled Structures, 2015, 89:178-191.
[8] Yao Z Y, Rasmussen K J. Finite Element Modelling and Parametric Studies of Perforated Thin-Walled
[9] Schafer, B.W., Local, Distortional and Euler Buckling of Thin-Walled Columns [J].Struct. Eng.2002, 128 (3): 289-299.
[10] Hancock, C.J., et al. Cold-formed steel structures to the AISI Specification. Marcel Dekker, New York, 2001.
[11] NAS (2007), North American Specification for the design of cold-formed steel structural members (AISI-S100-07), American Iron and Steel Institute (AISI), Washington DC.
[12] AS/NZS, Cold-formed steel structures, Standards of Australia and Standards of New Zealand. Sydney-Wellington; 2005.
[13] ABNT (2010), Design of cold-formed steel structures (ABNT NBR 14762:2010). Brazilian Association for Technical Specifications, Rio de Janeiro, R

Table 2: The finite element calculation results of the specimen under the eccentric load

Specimen	P_A / kN	Failure mode	Specimen	P_A / kN	Failure mode
C400-Ex5	162.05	D	C400-1Ex-5	145.84	L+F
C400-Ex10	136.69	D+F	C400-1Ex-10	129.91	L+F
C400-Ex20	104.12	D+F	C400-1Ex-20	106.85	L+F
C400-Ex30	83.88	D+F	C400-1Ex-30	90.15	L+F
C400-Ex40	69.64	D+F	C400-1Ex-40	78.57	L+F
C1000-Ex5	158.14	D+F	C1000-1Ex-5	138.52	L+F
C1000-Ex10	133.28	D+F	C1000-1Ex-10	121.42	L+F
C1000-Ex20	98.32	D+F	C1000-1Ex-20	98.73	L+F
C1000-Ex30	86.16	D+F	C1000-1Ex-30	84.09	L+F
C1000-Ex40	65.27	D+F	C1000-1Ex-40	73.72	L+F
C1600-Ex5	153.93	D+F	C1600-1Ex-5	120.95	L+F
C1600-Ex10	124.70	D+F	C1600-1Ex-10	104.15	L+F
C1600-Ex20	85.54	D+F	C1600-1Ex-20	86.19	L+F
C1600-Ex30	75.23	D+F	C1600-1Ex-30	73.12	L+F
C1600-Ex40	59.58	D+F	C1600-1Ex-40	64.66	L+F
C2200-Ex5	151.12	D+F	C2200-1Ex-5	99.15	L+F
C2200-Ex10	109.45	D+F	C2200-1Ex-10	86.52	L+F
C2200-Ex20	76.27	D+F	C2200-1Ex-20	71.78	L+F
C2200-Ex30	62.26	D+F	C2200-1Ex-30	66.08	L+F
C2200-Ex40	53.02	D+F	C2200-1Ex-40	54.93	L+F
C400-Ey5	165.72	D+F	C1000-1Ey5	157.26	D+L+F
C400-Ey10	152.19	D+L+F	C1000-1Ey10	145.39	D+L+F
C400-Ey20	134.81	D+L+F	C1000-1Ey20	124.77	D+L+F
C400-Ey30	118.35	D+L+F	C1000-1Ey30	109.50	D+L+F
C400-Ey40	105.39	D+L+F	C1000-1Ey40	98.94	D+L+F
C1600-Ey5	147.36	D+L+F	C2200-1Ey5	151.22	D+L+F
C1600-Ey10	136.98	D+L+F	C2200-1Ey10	129.86	D+L+F
C1600-Ey20	117.54	D+L+F	C2200-1Ey20	107.77	D+L+F
C1600-Ey30	100.77	D+L+F	C2200-1Ey30	93.15	D+L+F
C1600-Ey40	89.57	D+L+F	C2200-1Ey40	82.09	D+L+F
B400-Ex5	281.96	D	B400-Ey5	296.53	D
B400-Ex10	250.75	D	B400-Ey10	275.75	D
B400-Ex20	205.59	D	B400-Ey20	239.75	D
B400-Ex30	174.10	D	B400-Ey30	210.96	D
B400-Ex40	146.96	D	B400-Ey40	188.08	D
B1000-Ex5	300.68	D+ L+F	B1000-Ey5	333.58	D+ L+F
B1000-Ex10	267.61	D+ L+F	B1000-Ey10	289.49	D+ L+F
B1000-Ex20	218.38	D+ L+F	B1000-Ey20	249.70	D+ L+F
B1000-Ex30	181.95	D+ L+F	B1000-Ey30	221.42	D+ L+F
B1000-Ex40	155.90	D+ L+F	B1000-Ey40	199.07	D+ L+F
B1600-Ex5	290.86	D+ L+F	B1600-Ey5	302.16	D+ L+F
B1600-Ex10	245.60	D+ L+F	B1600-Ey10	271.23	D+L+F
B1600-Ex20	198.07	D+ L+F	B1600-Ey20	232.36	D+ L+F
B1600-Ex30	161.82	D+ L+F	B1600-Ey30	203.12	D+ L+F

B1600-Ex40	136.89	D+ L+F	B1600-Ey40	179.48	D+ L+F
B2200-Ex5	272.63	D+ L+F	B2200-Ey5	274.61	D+ L+F
B2200-Ex10	235.20	D+ L+F	B2200-Ey10	245.53	D+ L+F
B2200-Ex20	208.94	D+ L+F	B2200-Ey20	227.69	D+ L+F
B2200-Ex30	135.57	D+ L+F	B2200-Ey30	194.93	D+ L+F
B2200-Ex40	116.52	D+ L+F	B2200-Ey40	164.43	D+ L+F